Sustainable Food Technology

ROYAL SOCIETY OF CHEMISTRY

PAPER

View Article Online
View Journal



Cite this: DOI: 10.1039/d5fb00619h

# Edible chitosan–rice husk cellulose nanocrystal films and coatings with cinnamon *vs.* lemongrass essential oils: antifungal efficacy for mango anthracnose under tropical ambient storage

Namfon Samsalee,[a] Jitrawadee Meerasri,[b] Thidarat Bumrungpakdee,[a] María Bernardita Pérez-Gago[c] and Rungsinee Sothornvit *[d]

This study developed edible biocomposite films from chitosan–rice husk cellulose nanocrystals (CS–CNCs) with cinnamon essential oil (CEO) or lemongrass essential oil (LEO) (0.5–3% w/w). Films were characterized for physicochemical and antimicrobial properties, and coatings were assessed on inoculated mangoes under ambient tropical storage (32 °C). The presence of essential oil (EO) significantly increased film antioxidant activity, total phenolic content and antimicrobial properties. However, the tensile strength of the CS–CNC biocomposite films decreased from 19.39 ± 1.84 MPa to 4.54 ± 0.81 MPa at 3% CEO and to 1.62 ± 0.58 MPa at 2% LEO, and the elongation at break decreased from 12.07% ± 1.28% to 7.34% ± 0.67% and 2.49% ± 0.79%, respectively. Notably, 3% CEO improved the water vapour permeability (1.49 ± 0.16 g mm $kPa^{-1}$ $h^{-1}$ $m^{-2}$) of films compared with both the control film (without EO) (2.21 ± 0.05 g mm $kPa^{-1}$ $h^{-1}$ $m^{-2}$) and the 2% LEO containing film (2.41 ± 0.19 g mm $kPa^{-1}$ $h^{-1}$ $m^{-2}$). The CS–CNC-EO film-forming solutions demonstrated 100% mycelial growth inhibition of *Colletotrichum gloeosporioides* at ≥1% CEO and 2% LEO *in vitro*. When applied to mangoes, the coating treatments significantly retarded disease severity in inoculated fruits compared with the uncoated controls during storage. CS–CNC biocomposite films incorporated with 0.5% (w/w) CEO or LEO are effective in the reduction of the anthracnose disease of mango. Future development should focus on improving the sensory properties, controlling ingredient migration, and addressing scalability for industrial food packaging applications that can be adapted to other perishable fruits beyond mangoes while ensuring regulatory compliance and consumer acceptance.

Received 25th September 2025
Accepted 26th January 2026

DOI: 10.1039/d5fb00619h

rsc.li/susfoodtech



### Sustainability spotlight

This study reports the development of a sustainable biocomposite packaging film based on chitosan (CS) reinforced with rice husk-derived cellulose nanocrystals (CNCs) and incorporated with essential oils. The CS–CNC matrices containing cinnamon essential oil (CEO) or lemongrass essential oil (LEO) exhibited pronounced antifungal efficacy against *Colletotrichum gloeosporioides*, the anthracnose disease-causing pathogen in mango. The application of CS–CNC coatings supplemented with 0.5% CEO or LEO significantly delayed postharvest deterioration, thereby extending fruit storability. By valorizing rice husk, an abundant agro-industrial by-product, this work underscores the potential of biopolymer-based films as sustainable alternatives to synthetic polymers. The findings align with the United Nations Sustainable Development Goals (SDGs), particularly SDGs 2, 3, and 12, by promoting food security, human well-being, and responsible production.

## 1. Introduction

Packaging maintains food quality and prolongs the shelf life of perishable items, particularly those that are vulnerable to microbiological decay. The preparation of active packaging films is garnering increased attention from the food and packaging industries, driven by consumer demand for minimally processed and preservative-free products.[1] Renewable polysaccharides, such as cellulose, chitosan (CS), starch, and pectin, widely utilized in polysaccharide-based films possess favourable biocompatibility, biodegradability, and superior film-

[a]Department of Applied Biology, Faculty of Sciences and Liberal Arts, Rajamangala University of Technology Isan, Nakhon Ratchasima, 30000, Thailand
[b]Mahidol University-Frontier Research Facility (MU-FRF), Research Management and Development Division, Mahidol University, Salaya, Phuttamonthon, Nakhon Pathom, 73170, Thailand
[c]Postharvest Technology Center (CTP), Valencian Institute of Agrarian Research (IVIA), 46113 Montcada, Valencia, Spain
[d]Department of Food Engineering, Faculty of Engineering at Kamphaeng Saen, Kasetsart University, Kamphaeng Saen Campus, Nakhon Pathom, 73140, Thailand. E-mail: fengrns@ku.ac.th

forming properties, demonstrating significant potential for packaging applications.[2] Furthermore, they have been shown to effectively protect food products from the transmission of moisture, oxygen, and carbon dioxide, as well as light-induced chemical deterioration and microbial contamination, thus extending their shelf life.[3] CS is an affordable, non-toxic biopolymer with biocompatibility, biodegradability, and strong antimicrobial and antifungal properties.[4] However, pure CS films exhibit limited mechanical strength and poor barrier properties because of their hydrophilic nature.[5,6] Cellulose and its derivatives are the most abundant natural biopolymers and are widely used due to their renewable, biodegradable, non-toxic, and biocompatible properties.[7] In recent years, nanocellulosic materials, such as cellulose nanofibrils (CNFs), cellulose nanocrystals (CNCs), and bacterial cellulose, have attracted increasing attention due to their potential as natural nanofillers for the production of bio-nanocomposites. Their exceptional crystallinity, mechanical durability, thermal resistance, and biocompatibility have enabled their application as biodegradable packaging materials.[2,7] Pires *et al.*[8] reinforced CS films using a combination of extracted micro- and nanocellulose, which improved the mechanical, thermal, and barrier properties of these films. Khan *et al.*[9] demonstrated that CNC effectively reinforced CS films, leading to significant improvements in both mechanical and barrier properties. Specifically, only 5% CNC loading resulted in a 24% increase in tensile strength and a 27% reduction in water vapour permeability (WVP). These enhanced characteristics, attributed to strong filler–matrix interactions and homogeneous CNC dispersion, indicate that CNC-reinforced CS films are highly promising for food packaging applications.

Furthermore, the incorporation of essential oils may serve as an effective approach to reduce the WVP of films.[10] Natural essential oils are mixtures of volatile secondary metabolites derived from plants. Approximately 3000 have been identified in nature, of which about 10% are commercially used in foods, beverages, cosmetics, pharmaceuticals, aromatherapy, and sanitary products.[11] Their components include alcohols, esters, aldehydes, phenols, ethers, and ketones, among others, and many are classified as Generally Recognized as Safe (GRAS) by the U.S. Food and Drug Administration.[1,12] Lemongrass essential oil (LEO), extracted from the leaves of *Cymbopogon citratus*, primarily contains geranial (α-citral), neral (β-citral), and myrcene as its major constituents.[11] Cinnamon essential oil (CEO; *Cinnamomum zeylanicum*), a volatile compound extracted from bark, demonstrates a range of biological activities, including anti-inflammatory, antidiabetic, antioxidant, and antimicrobial properties.[13] The primary bioactive compounds in CEO are cinnamaldehyde, eugenol and linalool.[14,15] The prominent antimicrobial activity of CEO is attributed to cinnamaldehyde, its main bioactive constituent.[14,16] Numerous studies have reported that CEO and LEO exhibit antibacterial and antifungal properties. Moreover, Ojagh *et al.*[17] found that incorporating CEO into CS films reduced WVP by forming covalent bonds with CS, which decreased the availability of hydroxyl and amino groups and limited hydrogen bonding with water. Therefore, the incorporation of essential oils into composite films is considered an attractive strategy by packaging manufacturers and health-conscious consumers to prevent microbial food spoilage and enhance film properties.

Edible films and coatings are layers of edible materials that can be peeled off and consumed with food products. The key advantages of these films and coatings are that they are edible and biodegradable, as well as inexpensive, simple to manufacture, and environmentally friendly.[18] Moreover, the coating serves to create a layer with physical barrier and physiological inhibitory characteristics to maintain food quality.[19] Dip coating is a prevalent coating technique in comparison to brush and spray coating due to its ease of operation, efficiency, and labour-saving attributes.[20] In addition, the coating reduces peel permeability, modifies the internal atmosphere, minimizes water loss, and lowers the respiration rate of fruits.[21] Mango (*Mangifera indica* L.) is the world's second most economically valuable tropical fruit.[18] However, mangoes are highly perishable and susceptible to several postharvest diseases, posing major challenges to their commercial distribution. As a climacteric fruit, it undergoes rapid ripening, which leads to softening and increased vulnerability to microbial infections.[22,23] The major postharvest disease affecting mangoes in humid tropical regions is anthracnose caused by the fungus *Colletotrichum gloeosporioides*.[22,24] These postharvest constraints significantly limit storage, handling, and long-distance transport, thereby impeding global trade. Mango fruits infected with *Colletotrichum* spp. develop slightly black, sunken lesions that gradually enlarge, leading to fruit rot and undesirable changes in taste and odour; therefore, the most common treatment involves the use of chemical fungicides.[25] The disease has been effectively managed using various fungicides, including benomyl, mancozeb, carbendazim, azoxystrobin, thiophanate methyl, prochloraz, copper oxychloride, propineb, thiabendazole, and captan, which are widely employed to control anthracnose.[26,27] However, increasing concerns regarding environmental safety and human health have limited the use of these chemicals. To reduce the postharvest deterioration of mangoes, edible films or coatings have been extensively explored. For example, CEO, LEO, and basil essential oil exhibit antifungal activity against *Colletotrichum* spp., which are the causative agents of mango postharvest disease.[28] The incorporation of essential oils into edible coatings thus represents an effective alternative strategy for managing postharvest diseases. Edible coatings have emerged as sustainable alternatives that can delay ripening, improve appearance and extend shelf life at a low cost without being toxic or environmentally polluting.[29] In this context, the application of CS coatings has proven effective in reducing transpiration, firmness loss, and microbial decay while enhancing antioxidant capacity and improving the overall postharvest quality of fruit.[30]

Our previous work demonstrated that CNC derived from rice husks *via* chemical treatment combined with high-pressure homogenization exhibited high crystallinity (approximately 64–72%) and a high aspect ratio (approximately 37.40–39.13).[7] The CNC had a mean diameter of 11.94–12.34 nm and a mean length of 436.22–440.04 nm.[7] These structural characteristics

 

contributed to enhanced mechanical strength, improved water barrier performance, and increased stability of biopolymer packaging films.[7] Despite these promising results, there remains limited information on the functionalization of CS–CNC composites derived from rice husks with natural bioactive agents. To the best of our knowledge, no studies have reported the incorporation of CEO and LEO into CS–CNC matrices to develop functional films or coatings for mango preservation. Based on the characteristics of CNC (as a reinforcing nanofiller) and essential oils (as natural antimicrobial agents), it was hypothesized that the synergistic interaction between CS and CNC would enhance structural integrity and modulate the controlled release of essential oils by improving antifungal performance. Therefore, the present work aimed to develop and characterize CS–CNC-based films incorporated with varying concentrations of CEO and LEO and to evaluate their effectiveness as edible coatings in reducing anthracnose disease in mangoes.

## 2. Materials and methods

### 2.1 Materials

Rice husk, as an agricultural waste, was sourced from rice mills in Nakhon Pathom Province, Thailand. Chitosan (CS) food grade derived from shrimp shells (degree of deacetylation ≥ 90) was supplied by Marine BioResources Co., Ltd. (Samut Sakhon, Thailand). Mangoes at the mature green stage (110 days after fruit set) are obtained from orchards in Chachoengsao Province, Thailand. Acetic acid was purchased from QRëc™ (New Zealand). Sulfuric acid (37%) was procured from Thermo Fisher Scientific (Korea). Glycerol was obtained from Ajax Finechem Pty Ltd. (NSW, Sydney, Australia). Food-grade cinnamon essential oil (CEO) and lemongrass essential oil (LEO) were obtained by applying the steam distillation method and procured from Thai-China Flavours and Fragrances Industry Co., Ltd. (Nonthaburi, Thailand). Potato Dextrose Agar (PDA) and Mueller Hinton Agar (MHA) were obtained from HiMedia Laboratories Pvt. Ltd. (Maharashtra, India). Mancozeb (80% WP) was obtained from Suncrop Group Ltd. (Bangkok, Thailand). 2,2-Diphenyl-1-picrylhydrazyl (DPPH) and Folin–Ciocalteu reagent were purchased from Merck KGaA (Darmstadt, Germany). Trolox ((±)-6-hydroxy-2,5,7,8-tetramethylchromane-2-carboxylic acid) and gallic acid monohydrate were obtained from Sigma-Aldrich, St. Louis, MO, USA. All chemical reagents were of laboratory grade.

### 2.2 Preparation of chitosan–rice husk cellulose nanocrystal biocomposite films incorporated with essential oil

CNCs derived from rice husks used for biopolymer film-forming (1% w/w) were prepared according to the method of Samsalee *et al.*[7] A 1% (w/w) CS solution was prepared by dissolving CS flakes in a 1% (v/v) acetic acid solution, with continuous stirring for 2 h, followed by overnight incubation at 4 °C.[4] Glycerol (40% w/w of CS–CNC) as a plasticizer was added to the mixture while continuously stirring at 50 °C for 30 min.[31,32] The CNC suspension (1% w/w) was stirred at 50 °C for 30 min. Then, the CS and CNC solutions were mixed at a ratio of 40 : 60 (CS–CNC), which was selected from a previous study. The compositions of the prepared films are shown in Table 1. The solutions were mixed thoroughly using a high-speed homogenizer (Polytron PT3100D; Kinematica AG, Luzern, Switzerland) at 8000 rpm for 15 min.[31] Preparation of CS–CNC biocomposite films incorporating essential oil was carried out following the modified methodology of Samsalee and Sothornvit.[11] CEO or LEO was used at concentrations of 0.5%, 1%, 2%, and 3% w/w of the film-forming solution for this study.[33,34] Tween 80 was used as an emulsifier at concentrations of 25% for CEO and 50% for LEO to ensure emulsion stability in the CS–CNC film-forming system. The samples were homogenized using a high-speed homogenizer at 15 000 rpm for 3 min. Then, a mixing and defoaming machine (SK-300SII, Kakuhunter, Shiga, Japan) was used to reduce air bubbles in the mixture solution at 1800 rpm for 30 min. After pouring the film forming solution (90 g) onto a 13.5 cm diameter Petri dish, it was dried in a hot air oven at 50 °C for 16 h. The films were peeled off and stored in a controlled humidity chamber (25 ± 2 °C and 50% ± 5% relative humidity; RH) for at least 2 days before testing.

Table 1 Compositions of the novel chitosan–rice husk cellulose nanocrystal (CS–CNC) biocomposite films with different concentrations of cinnamon essential oil (CEO) or lemongrass essential oil (LEO)[a]

| Samples | CS, 1% w/w (g) | CNC, 1% w/w (g) | Gly (g) | EO (g) | TW80 (g) |
|---|---|---|---|---|---|
| CS–CNC | 40.00 | 60.00 | 0.40 | 0 | 0 |
| CS–CNC_0.5%CEO | 40.00 | 60.00 | 0.40 | 0.50 | 0.125 |
| CS–CNC_1%CEO | 40.00 | 60.00 | 0.40 | 1.00 | 0.250 |
| CS–CNC_2%CEO | 40.00 | 60.00 | 0.40 | 2.00 | 0.500 |
| CS–CNC_3%CEO | 40.00 | 60.00 | 0.40 | 3.00 | 0.750 |
| CS–CNC_0.5%LEO | 40.00 | 60.00 | 0.40 | 0.50 | 0.250 |
| CS–CNC_1%LEO | 40.00 | 60.00 | 0.40 | 1.00 | 0.500 |
| CS–CNC_2%LEO | 40.00 | 60.00 | 0.40 | 2.00 | 1.000 |

[a] CS = chitosan, CNC = cellulose nanocrystal, Gly = glycerol, EO = essential oil, TW80 = Tween 80.

### 2.3 Characterization of chitosan–rice husk cellulose nanocrystal biocomposite films incorporated with essential oil

**2.3.1 Colour of films.** The spectrophotometer (BYK Gardner GmbH, Geretsried, Germany) was calibrated using a white standard plate prior to measuring the colour of the films. The $L^*$, $a^*$, and $b^*$ values were recorded using a white standard background ($L^* = 86.23$, $a^* = -1.46$, and $b^* = 7.18$). The total colour difference ($\Delta E^*$) was then calculated using the following equation:

$$\Delta E^* = \sqrt{\left(L^* - L_0^*\right)^2 + \left(a^* - a_0^*\right)^2 + \left(b^* - b_0^*\right)^2},$$

where $L^*$, $a^*$, and $b^*$ represent the colour values of the film samples, and $L_0^*$, $a_0^*$, and $b_0^*$ represent the values of the white standard.

**2.3.2 Thickness of films.** Film thickness was measured using a hand-held micrometre (No. 7326, Mitutoyo Manufacturing Co., Ltd.; Tokyo, Japan) at five random points for each film. Three samples from each formula were tested.

**2.3.3 Water vapour permeability.** According to the ASTM E96 standard, the water vapour permeability (WVP) of the films was measured using the gravity method. Each test cup was filled with 6 mL of distilled water, sealed with a film sample, and then placed in a controlled environmental chamber at 27 ± 2 °C and 50% ± 5% relative humidity (RH). The cups were weighed at regular time intervals for 10 h. All measurements were conducted in triplicate for each film sample. The WVP was calculated by multiplying the water vapour transmission rate (WVTR) by the film thickness and dividing by the water vapour partial pressure difference across the film, as described by the following equation:

$$\mathrm{WVP} = \frac{\mathrm{WVTR} \times \mathrm{thickness}}{p_{A1} - p_{A2}},$$

where $p_{A1}$ and $p_{A2}$ denote the partial pressures of water vapour within and outside the cup, respectively.

**2.3.4 Mechanical properties.** Tensile strength (TS), elongation at break (EAB), and elastic modulus (EM) were measured using a Universal Testing Machine (Instron model 5569, MA, USA) following the ASTM D882-97 standard. The tests were conducted at 25 ± 2 °C and 50% ± 5% RH. Film specimens were cut to dimensions of 8 mm in width and 50 mm in length. The initial grip separation was set at 50 mm, with a crosshead speed of 10 mm $\mathrm{min}^{-1}$ and a load cell capacity of 50 N. Six replicates were tested for each film type.

**2.3.5 Total phenolic content.** Each film sample (0.20 ± 0.01 g) was mixed with 20 mL of distilled water and homogenized at 7000 rpm for 30 s. The resulting extract was centrifuged at 12 000*g* for 10 min at 25 °C. The clear supernatant was collected and used to determine the total phenolic content (TPC) and antioxidant activity using the DPPH assay.

The TPC of the films was determined using the Folin–Ciocalteu method, following the procedure described by Rodsamran and Sothornvit[35] with slight modifications. A 0.4 mL film extract was mixed with 2 mL of 10% Folin–Ciocalteu reagent and left at room temperature (25 °C) for 8 min, followed by the addition of 1.6 mL of 7.5% $Na_2CO_3$. The mixture was incubated in the dark for 1 h, and absorbance was measured at 765 nm using a spectrophotometer (V-770 UV/VIS/NIR, Jasco Corporation, Tokyo, Japan). A calibration curve prepared with gallic acid was used for quantification, and the results were expressed as milligrams of gallic acid equivalent (mg GAE) per gram of dry sample.

**2.3.6 Antioxidant activity based on the DPPH assay.** Antioxidant activity was evaluated using a DPPH radical scavenging assay. A 2 mL aliquot of the film extract was mixed with 2 mL of 50 μM DPPH in ethanol and incubated in the dark at room temperature for 1 h. Absorbance was measured at 515 nm using a spectrophotometer. The percentage of DPPH free radical scavenging activity was calculated using the following equation:

$$\text{DPPH free radical scavenging activity} = \frac{A_{\mathrm{control}} - A_{\mathrm{sample}}}{A_{\mathrm{control}}} \times 100\%$$

The DPPH radical scavenging activity was quantified based on a Trolox calibration curve and expressed as micromoles of Trolox equivalents per gram of dry sample (μmol Trolox per g).

**2.3.7 *In vitro* antimicrobial activity.** The antimicrobial activity of CS–CNC biocomposite films containing essential oils was evaluated using the disk diffusion method against representative Gram-positive bacteria (*Bacillus cereus* and *Bacillus subtilis*) and a Gram-negative bacterium (*Escherichia coli*). Mueller Hinton Agar (MHA) plates were inoculated with 100 μL of bacterial suspension ($1 \times 10^8$ CFU $\mathrm{mL}^{-1}$, 0.5 McFarland standard). Film samples were cut into 10 mm-diameter disks and sterilized under UV light for 20 min prior to placement on the inoculated agar surface.[36] The pure LEO or CEO of 20 μL was used to determine the efficiency of the essential oils. Plates were incubated at 37 °C for 24 h, and inhibition zones were measured as indicators of antimicrobial activity. Three replicates were performed for each treatment.

**2.3.8 *In vitro* antifungal activity.** The antifungal assay of each CS–CNC biocomposite film-forming solution incorporated with LEO or CEO was based on inhibition of radial mycelial growth of *C. gloeosporioides* on potato dextrose agar (PDA) using the poison food technique with a slight modification according to Klangmuang and Sothornvit.[22] Each PDA plate was supplemented with 10% (v/v) film-forming solution, while PDA without the solution served as the negative control. A PDA plate mixed with 2500 ppm mancozeb (a commercial fungicide) was used as a positive control. A 5 mm diameter plug of *C. gloeosporioides* (7–9 days old) was placed at the centre of each plate and incubated at 25 °C for 6 days. Radial mycelial growth was measured on days 4 and 6 as the average of two perpendicular colony diameters. Three replicates were performed for each treatment. The antifungal activity was expressed as the percentage of mycelial growth inhibition and was calculated using the following equation:

$$\text{Mycelial growth inhibition} = \frac{(d_c - d_t)}{d_c} \times 100,$$

where $d_c$ is the average diameter of mycelial growth on negative control plates and $d_t$ is the average diameter of mycelial growth of essential oil-treated film-forming solution plates and mancozeb plates.

**2.3.9 Fourier-transform infrared spectroscopy.** Fourier-transform infrared (FT-IR) spectra of the films were recorded using a Spectrum Two FTIR spectrometer (PerkinElmer Scientific, USA). Spectra were collected in the range of 4000–400 $\mathrm{cm}^{-1}$ with 16 scans at a resolution of 8 $\mathrm{cm}^{-1}$. Two replicates were performed per film.

**2.3.10 Morphology.** The surface and cross-sectional morphologies of the films were observed using a field emission scanning electron microscope (FE-SEM; Mira3, Tescan, Czech Republic) operated at 10 kV. Prior to scanning, the samples were coated with a thin layer of gold using a high-vacuum sputter coater (CCU-010, Safematic, Switzerland).

### 2.4 Application of edible coatings to 'Namdokmai Sithong' mangoes: effect on anthracnose development

Fresh 'Namdokmai Sithong' mangoes (*Mangifera indica* L.) at the mature green stage (110 days after fruit set) were obtained

from a local orchard. Uniform fruits (300–400 g) without visible defects or disease symptoms were selected. Fruits were disinfected by immersion in 0.05% (v/v) sodium hypochlorite solution for 5 min, rinsed with water, and air-dried in the laboratory. A cylindrical mango tissue sample (5 mm in diameter and 5 mm in depth) was removed from the centre of each fruit.[37] A 5 mm diameter mycelial plug of actively growing *C. gloeosporioides* was inserted into the wound and incubated overnight at room temperature before treatment. The experiment comprised 4 treatments, selecting the concentration of essential oil that was optimal in the evaluations of the films: (1) uncoated treatment (inoculated with *C. gloeosporioides*), (2) inoculated with *C. gloeosporioides* and then dipped in CS–CNC solution, (3) inoculated with *C. gloeosporioides* and then dipped in CS–CNC_0.5%CEO solution and (4) inoculated with *C. gloeosporioides* and then dipped in CS–CNC_0.5%LEO solution. Mangoes were dipped in the formulated coating solution for 30 s and then dried in a hot air oven at 40 °C for 30 min.[21] No visible heat injury or abnormal ripening behaviour was observed under these conditions. After treatment, the fruits were stored at 32 ± 1 °C for 9 days. Each treatment included three replicates, with three fruits per replicate. Every 3 days, disease severity was measured as the diameter of the lesion (mm).[37,38]

### 2.5 Statistical analysis

All experimental data were statistically analysed using a one-way analysis of variance, which was conducted with the IBM SPSS Statistics 23.0 software. Results were reported as mean ± standard deviation ($n \geq 3$). Duncan's multiple range test was used to determine significant differences among treatment means at the 95% confidence level ($p < 0.05$).

## 3. Results and discussion

### 3.1 Characterization of chitosan–rice husk cellulose nanocrystal biocomposite films incorporated with essential oil

**3.1.1 Colour of films.** Visual evaluation of CS–CNC biocomposite films with essential oils is crucial for assessing overall quality, appearance, and uniformity. This process involves examining the film surface for defects, such as cracks, and evaluating its colour and homogeneity. Fig. 1 shows the visual appearance of the CS–CNC biocomposite films containing different concentrations of CEO and LEO. CS–CNC films with CEO (0.5–3%) or LEO (0.5–2%) exhibited a slightly yellowish appearance. Due to the incorporation of plant essential oils into the polysaccharide film, the intensity of the yellow colour in the film increases.[39] Films with CEO (0.5–3%) demonstrated good uniformity and a more homogeneous appearance compared to those with 0.5%, 1% and 2% LEO.

However, none of the films presented visible cracks or bubbles. All formulations were easy to handle and peel from the casting plates, except for the film with 3% LEO, which displayed excessive brittleness, making it unsuitable for food packaging applications. Consequently, properties such as mechanical properties and water vapour permeability could not be evaluated for this film.

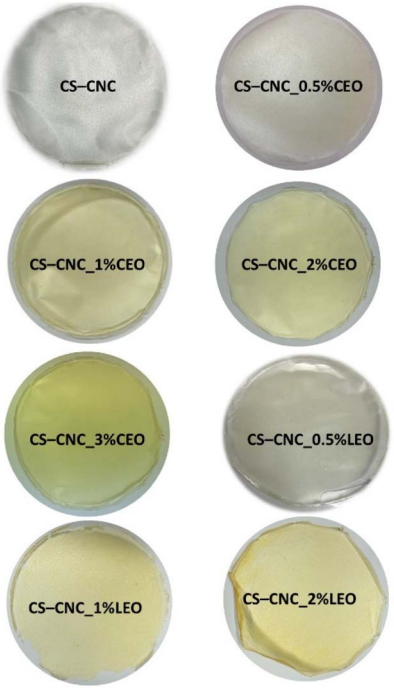


Fig. 1 Visual appearance of the novel chitosan–rice husk cellulose nanocrystal (CS–CNC) biocomposite films with different concentrations of cinnamon essential oil (CEO) or lemongrass essential oil (LEO).

Table 2 shows the colour parameters of CS–CNC films formulated with LEO and CEO. Films incorporated with LEO exhibited lower lightness ($L^*$) and greenness ($-a^*$) values but higher yellowness ($b^*$) and total colour difference values ($\Delta E^*$) compared to films with CEO at the same concentrations (except for $a^*$ value at 0.5% concentration). The addition of CEO or LEO at concentrations above 1% significantly reduced the $L^*$ and $a^*$ values compared to the films without essential oil (control films), while the $b^*$ and $\Delta E^*$ values increased. Notably, the $b^*$ values of films containing 0.5% LEO or CEO were not significantly different from the control likely due to the low concentration used. These findings indicate that both the concentration and type of essential oil affect the film's colour characteristics. This observation aligns with the findings of Song *et al.*,[40] who reported a slight yellow tint in corn and wheat starch films upon the addition of lime essential oil.

**3.1.2 Thickness of films.** Table 2 presents the effects of incorporating essential oils on the thickness of the CS–CNC biocomposite films. The film thickness ranged from 105.77 to 138.50 μm (Table 2). These films exhibited increased thickness with higher concentrations of either CEO or LEO, which may be associated with the higher surface solid density resulting from the film casting process. Furthermore, this phenomenon may be attributed to molecular interactions between the CS–CNC matrix and the active compounds in the essential oil. The primary active compounds found in CEO include eugenol and cinnamaldehyde,[15] while LEO primarily consists of geranial (α-citral) and neral (β-citral).[4,41] Such interactions could disrupt

Table 2 Colour parameters and thickness of the novel chitosan–rice husk cellulose nanocrystal (CS–CNC) biocomposite films with different concentrations of cinnamon essential oil (CEO) or lemongrass essential oil (LEO)[a]

| Samples | Colour | | | | Thickness (μm) |
|---|---|---|---|---|---|
| | $L^*$ | $a^*$ | $b^*$ | $\Delta E^*$ | |
| CS–CNC | $83.38 \pm 0.15^{c}$ | $-1.94 \pm 0.06^{c}$ | $14.50 \pm 0.55^{a}$ | $8.28 \pm 0.29^{a}$ | $105.77 \pm 0.95^{a}$ |
| CS–CNC_0.5%CEO | $85.57 \pm 0.51^{d}$ | $-1.01 \pm 0.22^{d}$ | $15.04 \pm 1.72^{a}$ | $12.33 \pm 1.80^{b}$ | $105.87 \pm 4.01^{a}$ |
| CS–CNC_1%CEO | $82.52 \pm 0.52^{b}$ | $-3.01 \pm 0.07^{b}$ | $23.60 \pm 2.98^{b}$ | $16.91 \pm 3.02^{c}$ | $109.57 \pm 2.30^{ab}$ |
| CS–CNC_2%CEO | $82.40 \pm 0.81^{b}$ | $-3.09 \pm 0.16^{b}$ | $24.02 \pm 4.91^{bc}$ | $17.20 \pm 5.08^{cd}$ | $111.60 \pm 1.57^{abc}$ |
| CS–CNC_3%CEO | $83.00 \pm 0.55^{bc}$ | $-3.44 \pm 0.06^{a}$ | $24.81 \pm 2.88^{bc}$ | $18.04 \pm 2.92^{cde}$ | $117.33 \pm 5.88^{c}$ |
| CS–CNC_0.5%LEO | $85.13 \pm 0.35^{d}$ | $-2.18 \pm 0.25^{c}$ | $17.46 \pm 1.56^{a}$ | $14.94 \pm 1.60^{bc}$ | $113.83 \pm 6.27^{bc}$ |
| CS–CNC_1%LEO | $80.98 \pm 0.35^{a}$ | $-2.02 \pm 0.11^{c}$ | $27.31 \pm 0.57^{bc}$ | $20.82 \pm 0.60^{de}$ | $133.23 \pm 5.46^{d}$ |
| CS–CNC_2%LEO | $81.40 \pm 0.73^{a}$ | $-2.08 \pm 0.33^{c}$ | $27.70 \pm 2.76^{c}$ | $21.10 \pm 2.84^{e}$ | $138.50 \pm 1.59^{d}$ |

[a] Mean ± standard deviation ($n = 3$). Different superscripts within a column indicate significant differences between means, as determined by the Duncan's multiple range test ($p < 0.05$).

polymer chain alignment, reduce network compactness, and consequently increase film thickness.[42] At the same concentration, the CS–CNC film containing LEO was significantly thicker than the CS–CNC film containing CEO ($p < 0.05$). Consistent with these findings, Ojagh *et al.*[17] reported that the thickness of the CS film increased with increasing CEO concentration (0, 0.4, 0.8, 1.5, and 2%v/v). Meanwhile, Wang *et al.*[43] observed that the addition of essential oils into CS films led to a looser microstructure and significantly greater thickness—up to fourfold for clove bud oil (10% w/w) and threefold for CEO (10% w/w).

**3.1.3 Water vapour permeability.** WVP reflects the rate at which water vapour passes through a film, which is crucial for its performance as a food packaging material. Films formulated with CEO were more effective at reducing WVP than those with LEO. Notably, films containing 2 and 3% CEO showed significantly lower WVP than the film without essential oils (CS–CNC), as shown in Table 3 ($p < 0.05$). In contrast, no significant differences were observed among the LEO-containing films at various concentrations compared to the control film. CS–CNC films with CEO had a WVP in the range of 1.49–1.95 g mm $kPa^{-1}$ $h^{-1}$ $m^{-2}$, while the control film was 2.21 g mm $kPa^{-1}$ $h^{-1}$ $m^{-2}$. This reduction in WVP may result from structural changes in the film, particularly the formation of a more compact or less porous structure during the evaporation of essential oils in the drying process. Some previous studies have reported that the incorporation of essential oils, including CEO, ginger essential oil and oregano essential oil, does not necessarily improve WVP.[12,44] A low WVP value is very important in coatings for fruits and vegetables because it helps to delay weight loss due to dehydration.[45]

**3.1.4 Mechanical properties.** The mechanical properties of CS–CNC films, with and without essential oils, are presented in Table 3. The addition of essential oils led to an increase in EM and a decrease in TS and EAB. Incorporating 0.5–1% LEO and 0.5–3% of CEO to the CS–CNC film resulted in higher EM values than the control film ($p < 0.05$). However, increasing the concentration of either essential oil reduced TS and EM. These results are consistent with findings by Hajirostamloo *et al.*,[46] who observed a TS reduction in soy protein isolate films upon adding cardamom essential oil microcapsules at increasing concentrations. Similarly, the addition of thyme essential oil at concentrations of 0–1.6% significantly reduced the TS of konjac glucomannan films.[47]

The observed decrease in mechanical performance is likely due to the disruption of the polymer matrix, resulting in non-uniform and discontinuous structures. Because essential oils have non-polar molecular structures and therefore possess hydrophobic properties,[41,48] their incorporation into

Table 3 Water vapour permeability (WVP) and mechanical properties of the novel chitosan–rice husk cellulose nanocrystal (CS–CNC) biocomposite films with different concentrations of cinnamon essential oil (CEO) or lemongrass essential oil (LEO)[a]

| Samples | WVP (g mm $kPa^{-1}$ $h^{-1}$ $m^{-2}$) | TS (MPa) | EM (MPa) | EAB (%) |
|---|---|---|---|---|
| CS–CNC | $2.21 \pm 0.05^{c}$ | $19.39 \pm 1.84^{f}$ | $171.40 \pm 13.92^{a}$ | $12.07 \pm 1.28^{c}$ |
| CS–CNC_0.5%CEO | $1.95 \pm 0.42^{abc}$ | $16.12 \pm 2.57^{e}$ | $925.28 \pm 42.95^{d}$ | $10.94 \pm 1.67^{c}$ |
| CS–CNC_1%CEO | $1.85 \pm 0.21^{abc}$ | $10.66 \pm 1.69^{d}$ | $908.62 \pm 33.15^{d}$ | $6.12 \pm 1.93^{b}$ |
| CS–CNC_2%CEO | $1.63 \pm 0.15^{ab}$ | $7.82 \pm 1.68^{c}$ | $506.34 \pm 93.75^{c}$ | $7.57 \pm 2.35^{b}$ |
| CS–CNC_3%CEO | $1.49 \pm 0.16^{a}$ | $4.54 \pm 0.81^{b}$ | $326.40 \pm 82.79^{b}$ | $7.34 \pm 0.67^{b}$ |
| CS–CNC_0.5%LEO | $2.19 \pm 0.59^{c}$ | $12.63 \pm 0.54^{d}$ | $605.79 \pm 97.05^{c}$ | $6.87 \pm 0.79^{b}$ |
| CS–CNC_1%LEO | $2.45 \pm 0.45^{c}$ | $8.02 \pm 1.00^{c}$ | $286.52 \pm 94.89^{b}$ | $4.01 \pm 0.99^{a}$ |
| CS–CNC_2%LEO | $2.41 \pm 0.19^{c}$ | $1.62 \pm 0.58^{a}$ | $157.54 \pm 51.60^{a}$ | $2.49 \pm 0.79^{a}$ |

[a] TS = Tensile strength; EM = elastic modulus; EAB = elongation at break (EAB). Mean ± standard deviation ($n = 3$ for WVP and $n = 6$ for mechanical properties). Different superscripts within a column indicate significant differences between means, as determined by the Duncan's multiple range test ($p < 0.05$).

 

hydrophilic polymer matrices alters the physical properties of the films.[48] The essential oils weaken polymer–polymer interactions by partially replacing them with weaker polymer–oil interactions, which involve non-polar hydrophobic interactions with the polymer chains and polar interactions with the CS–CNC matrix, resulting in a weakened network structure.[46,47,49]

Similarly, Perdones *et al.*[50] reported lower TS in lipid-containing films compared to lipid-free ones. However, the addition of CEO or LEO at concentrations of 1%, 2%, and 3% did not significantly change the EAB of the films as concentrations increased (Table 3) ($p > 0.05$). Furthermore, for the same concentration, films with LEO showed lower TS than those with CEO, suggesting different chemical interactions between essential oils and the polymer matrix.[51] This result can be further confirmed by FT-IR analysis.

**3.1.5 Total phenolic content.** The incorporation of CEO (1–3%) and LEO (1–2%) into CS–CNC films significantly increased TPC (Fig. 2). As expected, a higher essential oil concentration resulted in higher TPC values. However, films with 0.5% CEO or LEO showed no significant differences in TPC compared to the controls. Specifically, CEO addition at 0.5%, 1%, 2%, and 3% led to 2.61-, 5.61-, 7.83-, and 8.50-fold increases in TPC values, respectively, compared to the control. Conversely, LEO addition at 0.5%, 1%, and 2% increased TPC by 3.06-, 5.33-, and 10.00-fold, respectively, compared to the control films. According to the literature, CEO has a TPC of 70.8 mg GAE per g,[15] while LEO has 46.38 mg GAE per g [52] due to their respective compositions. CEO contains mainly eugenol (60.68%), cinnamaldehyde (33.94%) and linalool (1.29%),[15] whereas LEO contains citral (72.32%), myrcene (14.28%) and farsenol (10.37%).[53] Although LEO at 2% yielded the highest TPC, it was not significantly different from CEO at 2% and 3% ($p > 0.05$).

**3.1.6 Total antioxidant activity.** Fig. 3 shows the antioxidant activity of CS–CNC films added with CEO (0.5–3%) and LEO (0.5–2%). The control film had an antioxidant activity of 0.24 μmol (Trolox) per g dry sample. Previous studies have demonstrated the antioxidant activity of CS, which is attributed to the presence of nitrogen at the C2 of the polymeric structure.[54] The antioxidant activity of the films with CEO was in the range of 0.81–3.17 μmol (Trolox) per g dry sample, while LEO-added films were in the range of 1.15–2.74 μmol (Trolox) per g dry sample. Antioxidant activity increased with higher essential oil concentrations due to their phenolic content; however, no significant differences were observed among CEO (1–3%) or LEO (1–2%) concentrations. As expected, the TPC of the films is closely related to their antioxidant activity, as shown in Fig. 2 and 3. Therefore, CS–CNC biocomposite film integrated with CEO or LEO acts as an effectively active packaging material to maintain food quality and extend shelf life.

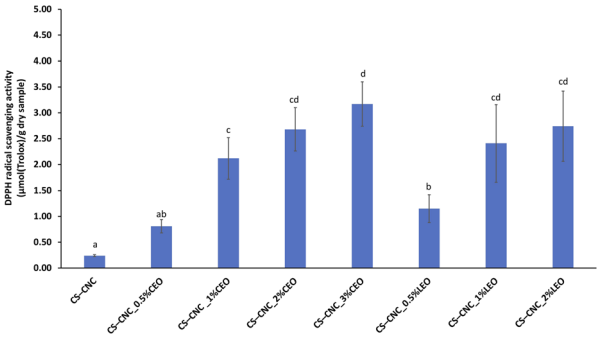


Fig. 3 Total antioxidant activity of the novel chitosan–rice husk cellulose nanocrystal (CS–CNC) biocomposite films with different concentrations of cinnamon essential oil (CEO) or lemongrass essential oil (LEO). Different letters represent significant differences ($p < 0.05$). The error bar shows the standard deviation.

**3.1.7 *In vitro* antimicrobial activity.** The two *in vitro* antimicrobial assays were intentionally designed to address different objectives. The antibacterial assay using UV-sterilized films aimed to evaluate the antimicrobial activity of the coating material in its solid form, while the antifungal assay using film-forming solutions incorporated into PDA was intended as a screening approach to assess the intrinsic antifungal potential of the active compounds prior to film application. UV exposure may affect volatile components and limit direct comparison with *in vivo* coating performance. These assays were therefore used as complementary screening tools, and the *in vivo* results provide a more realistic assessment of coating efficacy under practical conditions.

The antimicrobial activity of CEO and LEO was first evaluated independently before being incorporated into CS–CNC films since the effectiveness of each essential oil depends, among other factors, on the botanical origin and the extraction method. Both essential oils exhibited antimicrobial activity against *E. coli*, *B. cereus*, and *B. subtilis* (Table 4). LEO showed stronger antimicrobial activity against Gram-positive bacteria (*B. cereus* and *B. subtilis*) compared to CEO, while CEO showed effective antimicrobial activity against *E. coli*. These differences are attributed to the main active compounds. CEO contains cinnamaldehyde as its main active compound, which has demonstrated antibacterial activity against animal and plant diseases, foodborne pathogens, spoilage bacteria, and fungi.[16] LEO contains citral as its major component and has also demonstrated antibacterial activity against both Gram-negative and Gram-positive bacteria.[55] Furthermore, in line with our

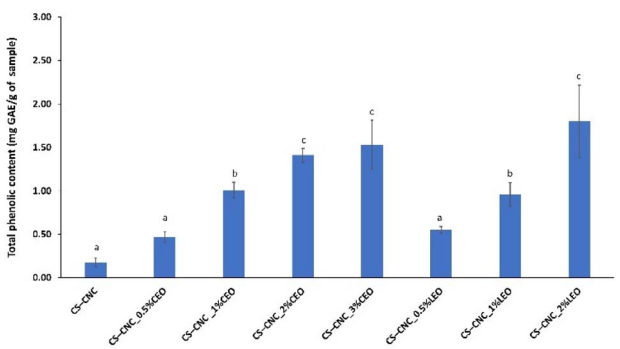


Fig. 2 Total phenolic content (TPC) of the novel chitosan–rice husk cellulose nanocrystal (CS–CNC) biocomposite films with different concentrations of cinnamon essential oil (CEO) or lemongrass essential oil (LEO). Different letters represent significant differences ($p < 0.05$). The error bar shows the standard deviation.

Table 4 Inhibition zone diameter (mm) of cinnamon essential oil (CEO) and lemongrass essential oil (LEO) against *Escherichia coli*, *Bacillus cereus* and *Bacillus subtilis*[a]

| Essential oil | *E. coli* | *B. cereus* | *B. subtilis* |
|---|---|---|---|
| CEO | $43.17 \pm 0.76^{b}$ | $50.67 \pm 1.76^{a}$ | $49.33 \pm 4.54^{a}$ |
| LEO | $15.14 \pm 0.29^{a}$ | $80.00 \pm 0.00^{b}$ | $76.33 \pm 3.51^{b}$ |

[a] The inhibition zone diameters were determined using undiluted (100%) essential oils. Mean ± standard deviation ($n = 3$). Different superscripts within a column indicate significant differences between means, as determined by a *t*-test ($p < 0.05$).

results, LEO was also found to be more effective against *B. cereus* than *E. coli*,[55] demonstrating that differences in bacterial cell wall structure affect the different antimicrobial effects of CEO and LEO against Gram-positive and Gram-negative bacteria.

In the case of the films, the CS–CNC film without essential oil showed no antimicrobial activity against Gram-negative (*E. coli*) and Gram-positive bacteria (*B. cereus* and *B. subtilis*) (Table 5), in agreement with previous studies.[33,56,57] Likewise, Wang *et al.*[43] reported no significant inhibition zone for pure CS films (2% w/w) against *E. coli*. Although the concentration of CS was higher than in this study, the CS films did not show any antimicrobial activity. This lack of activity may result from the limited diffusion of CS through the agar medium and strong polymer–polymer interactions.[43] Another possible explanation is that the inoculum level used in this study ($10^8$ CFU per Petri dish) was relatively high and may have surpassed the inhibitory capacity of CS. This observation is consistent with the findings of Zivanovic *et al.*,[58] who reported that CS films were unable to inhibit the bacterial growth of *L. monocytogenes* and *E. coli* at an inoculum level of $10^6$ CFU per Petri dish. Films containing 2% or 3% CEO and 1% or 2% LEO effectively inhibited *B. cereus*, with inhibition zones ranging from 15.50 to 17.60 mm. *B. subtilis* was inhibited by the CEO (1–3%) and 2% LEO, with similar inhibition zones (14.50–16.00 mm). No inhibition was observed against *E. coli* at any concentration. The general mode of action of essential oils inhibiting microbial growth is attributed to the high content of phenolic compounds, terpenes, alcohols, aldehydes, *etc.* These compounds are known to damage the phospholipid cell membrane of microorganisms, resulting in increased permeability and cytoplasmic leakage, or to interfere with enzymes located on the cell wall, which are essential for microbial metabolism.[58] In general, essential oils are slightly more effective against Gram-positive than Gram-negative bacteria.[57] This is related to the presence of an additional outer membrane surrounding the cell wall in Gram-negative bacteria (*E. coli*), which limits the diffusion of hydrophobic compounds through the lipopolysaccharide layer.[57] However, Hosseini *et al.*[59] reported that both the film preparation procedure and the structural characterization of the essential oil distribution in the film matrix significantly affected the antibacterial activity. The concentration and proportion of the active compounds in the essential oil affect its antibacterial activity, which depends on plant variety, origin, harvest time, and storage conditions.[58] Therefore, our results confirm that CS–CNC films incorporated with CEO and LEO enhanced antimicrobial activity against *B. cereus* and *B. subtilis*, highlighting their potential for use in active food packaging to prevent spoilage while maintaining quality and shelf life.

**3.1.8 *In vitro* antifungal activity.** Table 6 summarizes the antifungal activity of CS–CNC film-forming solutions (10% in PDA) against *C. gloeosporioides*. After 1 day of incubation, the radial mycelial growth was 8.50 mm, and on day 6, the mycelia showed complete fungal growth, while all solutions containing essential oils inhibited mycelial development. Complete (100%) inhibition was achieved with film-forming solutions containing 1–3% CEO and 2% LEO after 6 days of incubation. This suggests that the dispersion of the active compounds throughout the PDA medium increased their contact with the fungal cells, leading to enhanced inhibitory effects.[60] The study

Table 5 Inhibition zone diameter (mm) of the novel chitosan–rice husk cellulose nanocrystal (CS–CNC) biocomposite films with different concentrations of cinnamon essential oil (CEO) or lemongrass essential oil (LEO)[a]

| Samples | *E. coli* | *B. cereus* | *B. subtilis* |
|---|---|---|---|
| CS–CNC | nd | nd | nd |
| CS–CNC_0.5%CEO | nd | nd | nd |
| CS–CNC_1%CEO | nd | nd | $14.50 \pm 3.54^{a}$ |
| CS–CNC_2%CEO | nd | $16.17 \pm 3.33^{a}$ | $14.67 \pm 1.15^{a}$ |
| CS–CNC_3%CEO | nd | $15.50 \pm 2.60^{a}$ | $16.00 \pm 1.00^{a}$ |
| CS–CNC_0.5%LEO | nd | nd | nd |
| CS–CNC_1%LEO | nd | $16.70 \pm 4.55^{a}$ | nd |
| CS–CNC_2%LEO | nd | $17.60 \pm 3.29^{a}$ | $18.00 \pm 1.41^{a}$ |

[a] Mean ± standard deviation ($n = 3$). nd: no inhibition zone diameter was observed. Different superscripts within a column indicate significant differences between means, as determined by the Duncan's multiple range test ($p < 0.05$).

Table 6 Radial mycelial growth (mm) and percentage inhibition of *C. gloeosporioides* on Petri dishes of PDA amended with 10% novel chitosan–rice husk cellulose nanocrystal (CS–CNC) biocomposite film-forming solutions containing different concentrations of cinnamon essential oil (CEO) or lemongrass essential oil (LEO) after incubation at 25 °C[a]

| Samples | Mycelial growth (mm) | | Inhibition after 6 days (%) |
|---|---|---|---|
| | 4 days | 6 days | |
| Control | $47.50 \pm 1.70^{e}$ | $67.33 \pm 2.25^{e}$ | — |
| CS–CNC | $45.00 \pm 0.00^{e}$ | $71.67 \pm 3.21^{f}$ | $0.00 \pm 0.00^{a}$ |
| CS–CNC_0.5%CEO | $28.30 \pm 4.86^{c}$ | $42.00 \pm 6.28^{c}$ | $41.40 \pm 8.77^{c}$ |
| CS–CNC_1%CEO | $0.00 \pm 0.00^{a}$ | $0.00 \pm 0.00^{a}$ | $100 \pm 0.00^{e}$ |
| CS–CNC_2%CEO | $0.00 \pm 0.00^{a}$ | $0.00 \pm 0.00^{a}$ | $100 \pm 0.00^{e}$ |
| CS–CNC_3%CEO | $0.00 \pm 0.00^{a}$ | $0.00 \pm 0.00^{a}$ | $100 \pm 0.00^{e}$ |
| CS–CNC_0.5%LEO | $38.75 \pm 3.77^{d}$ | $54.00 \pm 1.15^{d}$ | $24.65 \pm 1.61^{b}$ |
| CS–CNC_1%LEO | $2.50 \pm 0.87^{b}$ | $25.50 \pm 0.50^{b}$ | $62.42 \pm 0.70^{d}$ |
| CS–CNC_2%LEO | $0.00 \pm 0.00^{a}$ | $0.00 \pm 0.00^{a}$ | $100 \pm 0.00^{e}$ |
| Mancozeb | $0.00 \pm 0.00^{a}$ | $0.00 \pm 0.00^{a}$ | $100.00 \pm 0.00^{e}$ |

[a] Mean ± standard deviation ($n = 3$). Different superscripts within a column indicate significant differences between means, as determined by the Duncan's multiple range test ($p < 0.05$).

demonstrated that all concentrations of essential oil investigated effectively inhibited mycelial growth, with greater concentrations resulting in higher efficacy. In addition, the type of essential oil used also affects its inhibitory effectiveness. The antifungal activity is attributed to the disruption of fungal cell membranes, leading to leakage of cytoplasmic contents and cell death.[22] Higher concentrations and the specific type of essential oil were associated with greater inhibitory effects. Furthermore, coating film-forming solutions containing 1–3% CEO and 2% LEO exhibited antifungal efficacy against *C. gloeosporioides* that was not significantly different from that of mancozeb (2500 ppm) ($p > 0.05$), a commercial fungicide used as the positive control. These results suggest that coating film-forming solutions containing CEO or LEO have strong potential as natural biocontrol agents against *C. gloeosporioides*.

**3.1.9 FT-IR spectra.** FT-IR analysis was used to examine the chemical interactions between CS–CNC and the essential oils at different concentrations. All the CS–CNC films blended with the essential oils had similar spectra (Fig. 4). The peaks in the wavenumber ranges of 3600–3000 $cm^{-1}$ and 2900–2800 $cm^{-1}$ showed slight shifts when essential oils were added, while the CS–CNC films without essential oil had peaks at wavenumbers of 3336.61 $cm^{-1}$ and 2881.01 $cm^{-1}$. However, the essential oils did not show any distinct peaks within these ranges. These observed peaks likely result from interactions between the –NH asymmetric stretching of CS and the O–H stretching vibrations of nanocellulose, as well as interactions between the C–H bonds of the methyl groups in CS and the C–H stretching vibrations of nanocellulose.[7,8] Prominent peaks of pure CEO were found at 1671.95 $cm^{-1}$, 1624.45 $cm^{-1}$, and 1120.46 $cm^{-1}$, corresponding to C═O, C═C and O–H stretching of aromatic compounds, such as aldehydes, phenols, and ketones, respectively. Peaks at 745.48 $cm^{-1}$ and 687.03 $cm^{-1}$ were linked to the C–H stretching vibrations of benzene rings and alkenes.[61] For LEO, the strong peak at 1672.63 $cm^{-1}$ was attributed to C═O stretching from the two aldehydes of neral and geranial.[62,63] Additionally, the low-intensity bands observed at 1439.47 $cm^{-1}$ and 1378.35 $cm^{-1}$ were ascribed to $-CH_3$ vibration absorption and the $-CH_2$ bending, respectively.[63] Therefore, the CS–CNC films with CEO exhibited more intense and sharper peaks in the 1636 – 1634 $cm^{-1}$ range compared to those with LEO. This may be due to stronger interactions between the functional groups in CEO (C═O and C═C) and the N–H bending vibrations in the CS–CNC matrix. These interactions may enhance peak distinctiveness and contribute to the greater mechanical strength of CS–CNC films containing CEO compared to those with LEO.

**3.1.10 Morphology.** The FE-SEM images in Fig. 5 show the surface and cross-sectional morphology of CS–CNC films with different concentrations of essential oils. The control CS–CNC film (without essential oil) showed a rough surface and brittle fracture on the cross-section, with stacked sheet-like structures. The addition of CNC enhances mechanical strength compared to pure CS films, but it also results in the film exhibiting brittle fracture characteristics in cross-section.[31] The rough surface appearance was maintained when CEO and LEO were incorporated into the CS–CNC films, while the cross-section revealed sheets stacked in compact layers, indicating that the essential oil was uniformly incorporated into the matrix. In addition, the cross-section of the films had voids and pores in its microstructure after the addition of the essential oil, which could be

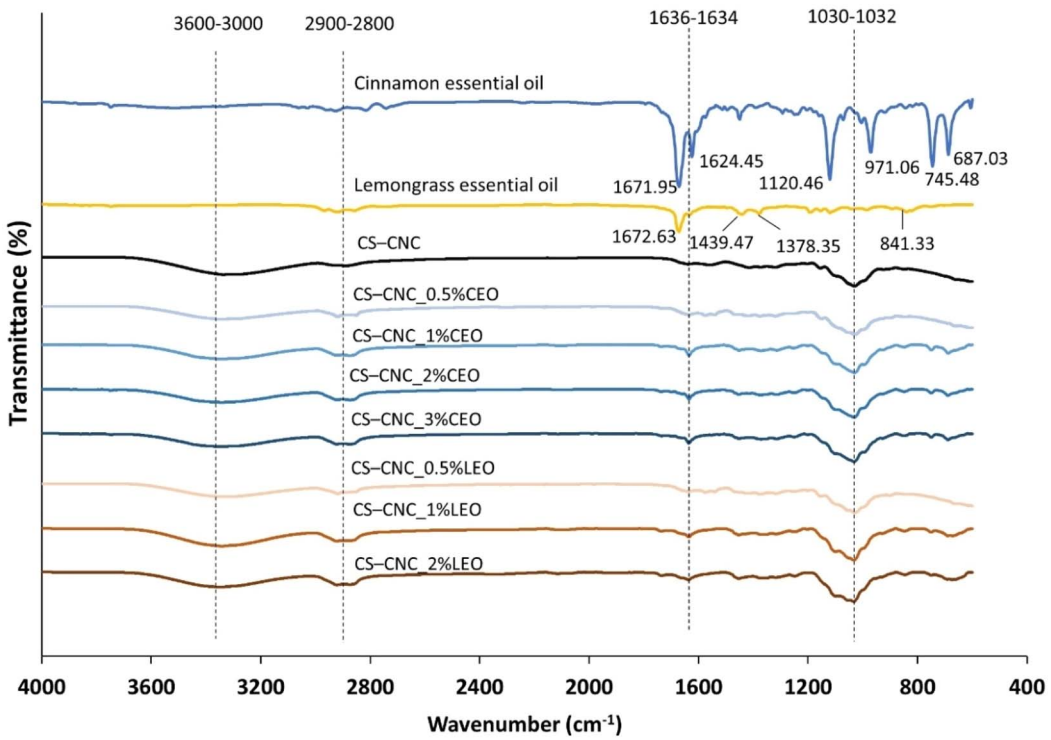


Fig. 4 FT-IR spectra of cinnamon essential oil (CEO), lemongrass essential oil (LEO) and the novel chitosan–rice husk cellulose nanocrystal (CS–CNC) biocomposite films with different concentrations of CEO or LEO.

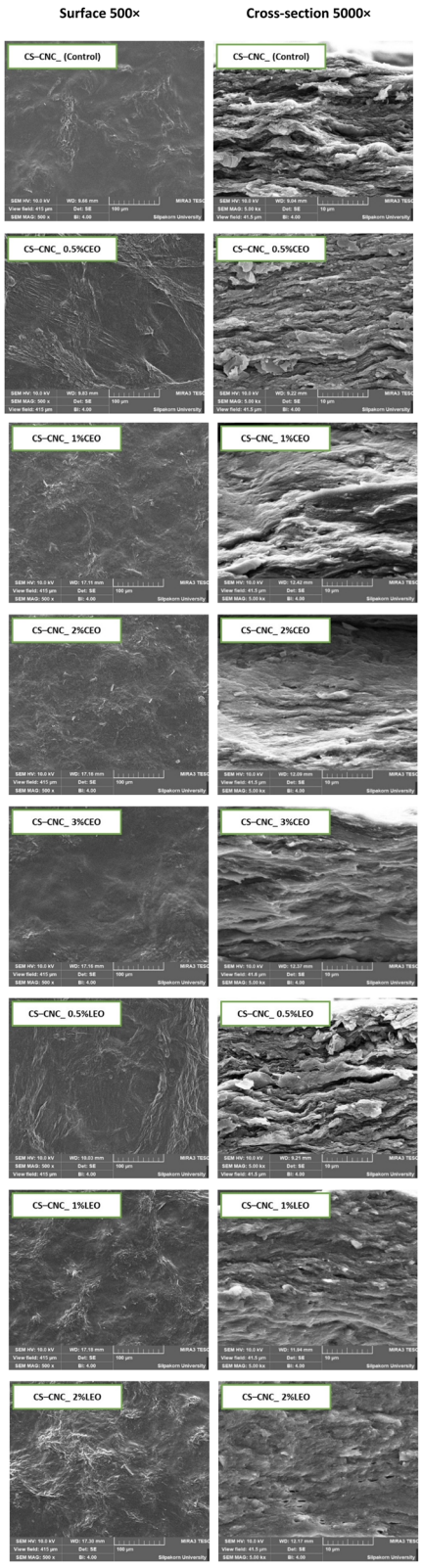


Fig. 5 FE-SEM images of the surface and cross-section of the novel chitosan–rice husk cellulose nanocrystal (CS–CNC) biocomposite films with different concentrations of cinnamon essential oil (CEO) or lemongrass essential oil (LEO).

due to the evaporation of the essential oil during film drying.[3] It was postulated that the film microstructure could be related to the reduction in tensile strength and higher WVP of films added with essential oils compared with the native film.[64]

### 3.2 Effect of edible coating on the 'Namdokmai Sithong' mango during storage

**3.2.1 Disease severity.** In this study, the wound inoculation method using a mycelial plug was selected to ensure uniform and reproducible infection pressure among samples, which is commonly used in postharvest pathology studies[22,38] to evaluate the protective efficacy of coatings under severe challenge conditions. This method does not fully replicate natural field infection routes, such as conidial deposition during flowering or fruit development, and the induced wound may accelerate disease development. However, it demonstrates the performance of active edible coatings under worst-case postharvest conditions rather than natural infection scenarios.

In the present study, a 0.5% essential oil (both CEO and LEO) was selected for edible coating applications on mangoes, as preliminary experiments showed that higher concentrations (above 0.5%) caused surface damage to the fruit during storage (Fig. S1). This aligns with previous findings that excessive essential oil concentrations can negatively impact fruit quality by inducing surface bruising and accelerating decay in fruits such as mangoes[65] and apples.[66] Fig. 6 shows the progression of disease symptoms of inoculated 'Namdokmai Sithong' mangoes stored at room temperature (32 ± 1 °C) over 9 days. After 3 days, uncoated mangoes developed significantly larger disease lesion diameters (20.63 mm) than coated mangoes (Fig. 6 and 7). After 6 days, both uncoated mangoes and CS–CNC coated mangoes had black spots, while mangoes coated with CS–CNC_0.5%CEO and CS–CNC_0.5%LEO displayed fewer signs of infection. Disease severity increased over time, reaching consumer-unacceptable levels after 9 days for uncoated fruit. However, mangoes coated with CS–CNC_0.5%CEO and CS–CNC_0.5%LEO showed only slightly visible dark spots on day 9. Disease lesion development measured every 3 days after

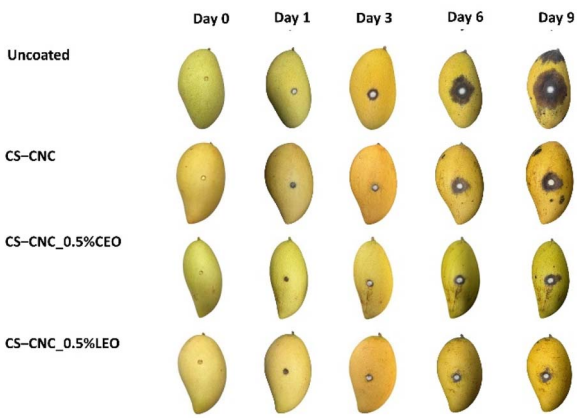


Fig. 6 Disease severity of inoculated 'Namdokmai Sithong' mangoes stored at room temperature (32 ± 1 °C) for 9 days under simulated tropical conditions.

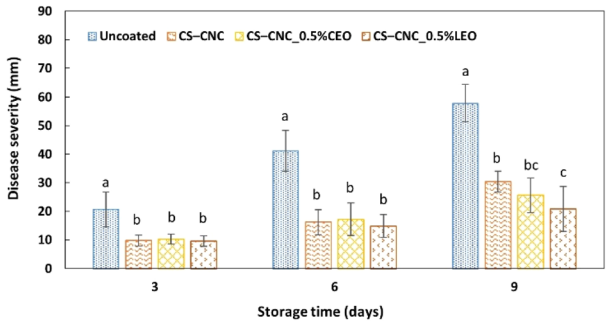


Fig. 7 Disease lesion diameter (mm) of inoculated 'Namdokmai Sithong' mango stored at room temperature (32 ± 1 °C) for 9 days. Vertical bars represent mean ± standard deviation. Different letters indicate significant differences during the same storage period ($p < 0.05$).

inoculation revealed that all coated treatments notably reduced disease severity throughout storage compared to the uncoated mango. These *in vivo* results are consistent with previous *in vitro* antifungal activities (Table 5), which showed that CS–CNC_0.5%CEO and CS–CNC_0.5%LEO film-forming solutions effectively inhibited *C. gloeosporioides*, the causal agent of anthracnose. By day 9, the uncoated mangoes exhibited extensive decay and a lesion diameter of approximately 57.83 mm. In contrast, mangoes coated with CS–CNC and CS–CNC_0.5% CEO had slightly scattered dark spots on the mango surface on day 9. Nevertheless, on day 9, mangoes treated with the CS–CNC_0.5% LEO had the smallest lesion diameter (20.82 mm), followed by those with CS–CNC_0.5%CEO (25.6 mm); the difference between them was not statistically significant. The antifungal efficiency of essential oils depends on their active compounds and concentrations, which contributed to the fungal inhibition observed. CEO contains cinnamaldehyde, while LEO mainly contains citral (α-citral and β-citral); both compounds possess conjugated aldehyde structures that contribute to their antifungal activity.[67,68] Therefore, the CS–CNC_0.5%CEO and CS–CNC_0.5%LEO coatings reduced the appearance of dark spots, improving the postharvest quality and marketability of mangoes. These findings are consistent with Jongsri *et al.*,[38] who reported that a combination of 1% CS and 0.1 ppm spermidine delayed ripening and reduced deterioration in mangoes. Similarly, CS-based formulations, either alone or in combination with active compounds, have been shown to minimize weight loss and extend mango shelf life.[23] In addition, previous research has investigated the development of edible films and coatings incorporating essential oils for postharvest pathogen control. For example, Maqbool *et al.*[69] observed that the combination of LEO and CEO with an edible coating from gum arabic showed effective control of *C. gloeosporioides* in papaya.

## 4. Conclusions

CS–CNC biocomposite films containing CEO and LEO at concentrations of 0.5, 1, 2, and 3% (w/w) were prepared using the solvent casting method. Their physicochemical and antimicrobial properties were subsequently evaluated. The incorporation of CEO and LEO increased the yellowness and greenness of the films. Both types of essential oil-enhanced films exhibited antibacterial activity against *B. cereus* and *B. subtilis* and effectively inhibited the mycelial growth of *C. gloeosporioides*. Moreover, the films added with CEO and LEO had good antioxidant activity (0.81–3.17 μmol Trolox per g dry sample), indicating their potential use as active packaging materials. The WVP values of films containing CEO were in the range of 1.49–1.95 g mm $kPa^{-1}$ $h^{-1}$ $m^{-2}$, which was significantly lower than films containing LEO or without essential oils. The addition of essential oils led to a reduction in tensile strength (from 19.39 MPa to 1.62–16.12 MPa) and elongation at break (from 12.07% to 2.49–10.94%); however, the elastic modulus increased relative to the control films (from 171.40 to 286.52–925.28 MPa), except for 2% LEO. Interestingly, films with CEO showed better mechanical performance than those with LEO, a result further supported by FT-IR analysis. When applied as edible coatings on inoculated mangoes, the CS–CNC films with essential oils significantly reduced black spot severity and disease severity compared to uncoated mangoes. Therefore, CS–CNC-based coatings enriched with essential oils show an alternative cost-effective and sustainable strategy to reduce global food waste. Future studies should focus on sensory evaluation, coating migration, coated fruit quality (*e.g.*, mass loss, firmness, soluble solids content, and titratable acidity), and scalability for industrial food packaging applications while ensuring regulatory compliance and consumer acceptance.

## Author contributions

Namfon Samsalee: conceptualization; funding acquisition; methodology; investigation; project administration; writing original draft; writing – review & editing. Jitrawadee Meerasri: methodology; investigation. Thidarat Bumrungpakdee: methodology; investigation. María Bernardita Pérez-Gago: methodology; supervision. writing – review & editing. Rungsinee Sothornvit: conceptualization; investigation; supervision; funding acquisition; writing – review & editing, resources.

## Conflicts of interest

The authors have no conflicts of interest to declare.

## Data availability

Data will be made available on request.

Supplementary information (SI): mangoes coated with CS–CNC films containing 1% CEO or LEO exhibited surface damage, evidenced by brown burn marks after 1 day of storage at room temperature. See DOI: https://doi.org/10.1039/d5fb00619h.

## Acknowledgements

This research project is supported by the National Research Council of Thailand (NRCT) through the Research Team

Promotion Grant/Senior Research Scholar (Grant No. N42A650552). We would like to acknowledge the Faculty of Sciences and Liberal Arts, Rajamangala University of Technology Isan and Faculty of Engineering at Kamphaeng Saen, Kasetsart University, Kamphaeng Saen Campus for facilities and support.

## References

1 P. López, C. Sánchez, R. Batlle and C. Nerín, *J. Agric. Food Chem.*, 2007, **55**(21), 8814–8824.
2 X. Chen, W. Lan and J. Xie, *Food Chem.*, 2024, **441**, 138343.
3 N. Samsalee and R. Sothornvit, *Food Bioprocess Technol.*, 2020, **13**(3), 488–500.
4 N. Samsalee and R. Sothornvit, *Food Packag. Shelf Life*, 2019, **22**, 100406.
5 C. Caner, P. J. Vergano and J. L. Wiles, *J. Food Sci.*, 1998, **63**, 1049–1053.
6 M. Mujtaba, R. E. Morsi, G. Kerch, M. Z. Elsabee, M. Kaya, J. Labidi and K. M. Khawar, *Int. J. Biol. Macromol.*, 2019, **121**, 889–904.
7 N. Samsalee, J. Meerasri and R. Sothornvit, *Carbohydr. Polym. Technol. Appl.*, 2023, **6**, 100353.
8 J. R. Pires, V. G. Souza, L. A. Gomes, I. M. Coelhoso, M. H. Godinho and A. L. Fernando, *Ind. Crops Prod.*, 2022, **186**, 115247.
9 A. Khan, R. A. Khan, S. Salmieri, C. Le Tien, B. Riedl, J. Bouchard, G. Chauve, V. Tan, M. R. Kamal and M. Lacroix, *Carbohydr. Polym.*, 2012, **90**(4), 1601–1608.
10 P. Tongnuanchan, S. Benjakul and T. Prodpran, *Food Chem.*, 2012, **134**(3), 1571–1579.
11 N. Samsalee and R. Sothornvit, *Int. J. Food Sci. Technol.*, 2019, **54**(9), 2745–2753.
12 A. Aguirre, R. Borneo and A. E. Leon, *Food Biosci.*, 2013, **1**, 2–9.
13 F. Esmaeili, M. Zahmatkeshan, Y. Yousefpoor, H. Alipanah, E. Safari and M. Osanloo, *BMC Complementary Med. Ther.*, 2022, **22**, 143.
14 N. Matan, H. Rimkeeree, A. J. Mawson, P. Chompreeda, V. Haruthaithanasan and M. Parker, *Int. J. Food Microbiol.*, 2006, **107**(2), 180–185.
15 R. M. Yitbarek, H. Admassu, F. M. Idris and E. G. Fentie, *Appl. Biol. Chem.*, 2023, **66**, 47.
16 Y. C. Wong, M. Y. Ahmad-Mudzaqqir and W. A. Wan-Nurdiyana, *Orient. J. Chem.*, 2014, **30**(1), 37–47.
17 S. M. Ojagh, M. Rezaei, S. H. Razavi and S. M. H. Hosseini, *Food Chem.*, 2010, **122**(1), 161–166.
18 E. Tavassoli-Kafrani, M. V. Gamage, L. F. Dumée, L. Kong and S. Zhao, *Crit. Rev. Food Sci. Nutr.*, 2022, **62**(9), 2432–2459.
19 T. Wang, X. Zhai, X. Huang, Z. Li, X. Zhang, X. Zou and J. Shi, *Food Packag. Shelf Life*, 2023, **39**, 101133.
20 Y. Zhong, G. Cavender and Y. Zhao, *LWT–Food Sci. Technol.*, 2014, **56**(1), 1–8.
21 P. S. Tanada-Palmu and C. R. Grosso, *Postharvest Biol. Technol.*, 2005, **36**(2), 199–208.
22 P. Klangmuang and R. Sothornvit, *J. Agric. Nat. Resour.*, 2022, **56**(2), 331–342.
23 N. Parvin, A. Rahman, J. Roy, M. H. Rashid, N. C. Paul, M. A. Mahamud, S. Imran, M. A. Sakil, F. M. J. Uddin, M. E. Molla, M. A. Khan, M. H. Kabir and M. A. Kader, *Horticulturae*, 2023, **9**(1), 64.
24 S. Diskin, T. Sharir, O. Feygenberg, D. Maurer and N. Alkan, *Crop Prot.*, 2019, **124**, 104855.
25 T. Tangpao, N. Phuangsaujai, S. Kittiwachana, D. R. George, P. Krutmuang, B. Chuttong and S. R. Sommano, *Agriculture*, 2022, **12**(9), 1407.
26 L. Chit-aree, Y. Unpaprom, R. Ramaraj and M. Thirabunyanon, *Biomass Convers. Biorefin.*, 2023, **13**(12), 10735–10749.
27 Y. Peralta-Ruiz, C. Rossi, C. D. Grande-Tovar and C. Chaves-López, *J. Fungi*, 2023, **9**(6), 623.
28 L. T. Danh, B. T. Giao, C. T. Duong, N. T. T. Nga, D. T. K. Tien, N. T. Tuan, B. T. C. Huong, T. C. Nhan and D. T. X. Trang, *Membranes*, 2021, **11**(9), 719.
29 M. Sanchez-Tamayo, J. L. Plaza-Dorado and C. Ochoa-Martínez, *Food Sci. Nutr.*, 2024, **12**(12), 10646–10654.
30 Y. Wang, Z. Yan, W. Tang, Q. Zhang, B. Lu, Q. Li and G. Zhang, *Horticulturae*, 2021, **7**(12), 518.
31 N. Samsalee, J. Meerasri and R. Sothornvit, *Packag. Technol. Sci.*, 2026, **39**(2), 125–136.
32 Y. H. How, E. M. Y. Lim, I. Kong, P. E. Kee and L. P. Pui, *Sustainable Food Technol.*, 2024, **2**(2), 400–414.
33 Q. Ma, Y. Zhang, F. Critzer, P. M. Davidson, S. Zivanovic and Q. Zhong, *Food Hydrocolloids*, 2016, **52**, 533–542.
34 F. N. Nkede, A. A. Wardana, N. T. H. Phuong, M. Takahashi, A. Koga, M. H. Wardak, M. Fanze, F. Tanaka and F. Tanaka, *J. Polym. Environ.*, 2023, **31**(11), 4930–4945.
35 P. Rodsamran and R. Sothornvit, *Food Chem.*, 2018, **242**, 239–246.
36 S. Sharma, S. Barkauskaite, B. Duffy, A. K. Jaiswal and S. Jaiswal, *Foods*, 2020, **9**(8), 1117.
37 T. Chuacharoen and C. M. Sabliov, *J. Agric. Food Res.*, 2022, **10**, 100444.
38 P. Jongsri, P. Rojsitthisak, T. Wangsomboondee and K. Seraypheap, *Sci. Hortic.*, 2017, **224**, 180–187.
39 F. Han Lyn and Z. A. Nur Hanani, *J. Packag. Technol. Res.*, 2020, **4**(1), 33–44.
40 X. Song, G. Zuo and F. Chen, *Int. J. Biol. Macromol.*, 2018, **107**, 1302–1309.
41 F. R. Procopio, R. P. Brexó, G. S. Martins, C. W. Fukuyama, M. E. da Mata Martins, S. Bogusz Junior and M. D. Ferreira, *Food Bioprocess Technol.*, 2025, **18**(10), 8788–8805.
42 V. G. L. Souza, J. R. A. Pires, C. Rodrigues, P. F. Rodrigues, A. Lopes, R. J. Silva, J. Caldeira, M. P. Duarte, F. B. Fernandes and A. L. Fernando, *Coatings*, 2019, **9**(11), 700.
43 L. Wang, F. Liu, Y. Jiang, Z. Chai, P. Li, Y. Cheng, H. Jing and X. Leng, *J. Agric. Food Chem.*, 2011, **59**(23), 12411–12419.
44 L. Atare's, C. De Jesu's, P. Talens and A. Chiralt, *J. Food Eng.*, 2010, **99**, 384–391.
45 M. Cortés-Rodríguez, C. Villegas-Yépez, J. H. G. González, P. E. Rodríguez and R. Ortega-Toro, *Heliyon*, 2020, **6**(9), e04884.

 

46 B. Hajirostamloo, M. Molaveisi, P. Jafarian Asl and M. M. Rahman, *J. Food Meas. Charact.*, 2023, **17**(1), 324–336.
47 Z. Liu, D. Lin, R. Shen, R. Zhang, L. Liu and X. Yang, *Food Packag. Shelf Life*, 2021, **29**, 100700.
48 S. Sharma, S. Barkauskaite, A. K. Jaiswal and S. Jaiswal, *Food Chem.*, 2021, **343**, 128403.
49 C. D. Grande-Tovar, A. Serio, J. Delgado-Ospina, A. Paparella, C. Rossi and C. Chaves-López, *J. Food Sci. Technol.*, 2018, **55**(10), 4256–4265.
50 Á. Perdones, M. Vargas, L. Atarés and A. Chiralt, *Food Hydrocolloids*, 2014, **36**, 256–264.
51 K. Venkatachalam, N. Rakkapao and S. Lekjing, *Membranes*, 2023, **13**(2), 161.
52 G. C. Njoku, C. V. Alisigwe, D. U. Iloanusi and P. C. Aririguzo, *Int. J. Innov. Sci. Res. Technol.*, 2022, **7**, 127–138.
53 J. Moncada, J. A. Tamayo and C. A. Cardona, *Ind. Crops Prod.*, 2014, **54**, 175–184.
54 M. A. López-Mata, S. Ruiz-Cruz, N. P. Silva-Beltrán, J. D. J. Ornelas-Paz, V. M. Ocaño-Higuera, F. Rodríguez-Félix, L. A. Cira-Chávez, C. L. Del-Toro-Sánchez and K. Shirai, *Int. J. Polym. Sci.*, 2015, **1**, 974506.
55 M. I. Perdana, J. Ruamcharoen, S. Panphon and M. Leelakriangsak, *LWT–Food Sci. Technol.*, 2021, **141**, 110934.
56 M. Mohammadi, S. Mirabzadeh, R. Shahvalizadeh and H. Hamishehkar, *Int. J. Biol. Macromol.*, 2020, **149**, 11–20.
57 F. M. Pelissari, M. V. Grossmann, F. Yamashita and E. A. G. Pineda, *J. Agric. Food Chem.*, 2009, **57**(16), 7499–7504.
58 S. Zivanovic, S. Chi and A. F. Draughon, *J. Food Sci.*, 2005, **70**(1), M45–M51.
59 M. H. Hosseini, S. H. Razavi and M. A. Mousavi, *J. Food Process. Preserv.*, 2009, **33**(6), 727–743.
60 K. Monzón-Ortega, M. Salvador-Figueroa, D. Gálvez-López, R. Rosas-Quijano, I. Ovando-Medina and A. Vázquez-Ovando, *J. Food Sci. Technol.*, 2018, **55**, 4747–4757.
61 E. Abedi, M. Sayadi and N. Oliyaei, *Int. J. Biol. Macromol.*, 2024, **266**, 131173.
62 E. P. da Cruz, J. B. Pires, F. N. dos Santos, L. M. Fonseca, M. Radünz, J. D. Magro, E. A. Gandra, E. D. R. Zavareze and A. R. G. Dias, *Food Hydrocolloids*, 2023, **145**, 109105.
63 M. Râpă, T. Zaharescu, L. M. Stefan, C. Gaidău, I. Stănculescu, R. R. Constantinescu and M. Stanca, *Polymers*, 2022, **14**(18), 3884.
64 S. F. Hosseini, M. Rezaei, M. Zandi and F. Farahmandghavi, *Ind. Crops Prod.*, 2015, **67**, 403–413.
65 M. D. Lieu, N. N. H. Ngo, T. L. Lieu, K. T. Nguyen and T. K. T. Dang, *Vietnam J. Sci. Technol.*, 2018, **56**(4), 458–467.
66 M. A. Rojas-Graü, R. M. Raybaudi-Massilia, R. C. Soliva-Fortuny, R. J. Avena-Bustillos, T. H. McHugh and O. Martín-Belloso, *Postharvest Biol. Technol.*, 2007, **45**(2), 254–264.
67 S. Y. Wang, P. F. Chen and S. T. Chang, *Bioresour. Technol.*, 2005, **96**(7), 813–818.
68 S. Tadtong, R. Chantavacharakorn, S. Khayankan, P. Akachaipaibul, W. Eiamart and W. Samee, *Int. J. Mol. Sci.*, 2025, **26**(12), 5601.
69 M. Maqbool, A. Ali, P. G. Alderson, M. T. M. Mohamed, Y. Siddiqui and N. Zahid, *Postharvest Biol. Technol.*, 2011, **62**(1), 71–76.